Monatshefte für Chemie 138, 453–464 (2007)
DOI 10.1007/s00706-007-0625-2
Printed in The Netherlands

Monatshefte für Chemie
Chemical Monthly

Synthesis and Photo Physical Properties of 9,10-Bis(hydroxyphenyl)anthracene Derivatives

Mischa Zelzer[1], **Stefan Kappaun**[1], **Egbert Zojer**[2], and **Christian Slugovc**[1,*]

[1] Institute of Chemistry and Technology of Organic Materials, Graz University of Technology, Graz, Austria
[2] Institute of Solid State Physics, Graz University of Technology, Graz, Austria

Received November 7, 2006; accepted (revised) November 19, 2006; published online April 20, 2007

Summary. Among the most promising fluorescent materials for sensor applications, anthracene and its derivatives have been widely studied. In this contribution, the synthesis and characterization of a series of isomers of bis(hydroxyphenyl)anthracene derivatives are described. The preparation of the corresponding derivatives *via Suzuki* cross-coupling reactions is presented with particular emphasis on finding appropriate protecting groups and studying the influence of the position of the hydroxy group on the outcome of the reaction. Moreover, the effects of protonation and deprotonation on absorption and emission spectra are reported and correlated to semi-empirical quantum mechanical calculations.

Keywords. Sensors; Semiempirical calculations; Protonation; Fluorescence spectroscopy; Absorption spectra.

Introduction

The design, synthesis, and characterization of fluorescent materials with photo physical properties altered by external stimuli are a field of intense research [1]. Due to the high sensitivity and low-cost instrumentation of fluorescence spectroscopy, numerous fluorophores are already used as reporter molecules for labeling and sensing purposes in a variety of areas such as medicine or environmental monitoring [2]. Although extensive work has been devoted to the design and characterization of fluorescent materials with a sensing function, only few classes of molecules fulfill the criteria for practical applications [1c]. Further, the development of advanced analytical techniques (*e.g.* multiphoton microscopy) requires fluorophores meeting even more specific criteria [3] and, thus, boosts scientific efforts to identify suitable classes of materials with adequate material properties.

Among the most promising fluorescent materials for sensor applications, anthracene and its derivatives have been intensely studied because of their excellent photoluminescence (PL) characteristics and planar conjugated backbone [4]. Utilizing these desirable properties, a series of fluorescence sensors especially for metal ions and biological molecules has been realized [1a, 4a, 5]. Nevertheless, investigations on hydroxy functionalized anthracene derivatives and the influence of deprotonation on their photo physical properties are rare [6].

As a further advance in the design of anthracene based sensor materials, in this contribution we report on the preparation and characterization of 9,10-bis(hydroxyphenyl)anthracene derivatives. Three different derivatives, namely 9,10-bis(4-hydroxyphenyl)anthracene (**6**), 9,10-bis(3-hydroxyphenyl)anthracene (**10**), and 9,10-bis(2-hydroxyphenyl)anthracene (**11**) are discussed. We present procedures for their synthesis, and demonstrate the impact of deprotonation on absorption and emission spectra of the corresponding materials. The latter aims at establishing a correlation between *pH*-dependent luminescence properties and molecular structure. To provide deeper insight into the effects of deprotonation on the

* Corresponding author. E-mail: slugovc@tugraz.at

microscopic electronic structure of these 9,10-bis(hydroxyphenyl)anthracenes, semi-empirical quantum mechanical calculations are enclosed and allow a conclusive interpretation of the experimental data.

Results and Discussion

The presented strategy for the synthesis of 9,10-bis(hydroxyphenyl)anthracenes makes use of boronic acids obtained from the corresponding bromophenole **1** coupled with 9,10-dibromoanthracene (**4**) *via* a *Suzuki* cross-coupling reaction (*cf.* Scheme 1). While this approach offers the clear advantage of high functional group tolerance concerning the *Suzuki* cross-coupling reaction [7], more attention has to be paid to the preparation of the boronic acids. Due to the harsh conditions applied during their synthesis, a careful choice of protecting groups for the hydroxy functionality is essential. Thus, for the preparation of the corresponding 9,10-bis(hydroxyphenyl)anthracene derivatives a de-protection step subsequent to the *Suzuki* cross-coupling reaction is necessary, as reported by *Chung et al.* for the preparation of 9,10-bis(4-hydroxyphenyl)anthracene (**6**) [8]. Although protection of the hydroxy-function could be accomplished with several protecting groups in good to excellent yields (*e.g.* utilizing acetyl, pyran or benzyloxy groups), only the benzyloxy protected derivative gave in our hands the corresponding 4-benzyloxyphenylboronic acid (**3**) without the formation of undesired by-products in a yield of 80% (*cf.* Scheme 1) [9].

Besides the choice of the protecting group, the reaction conditions applied for the *Suzuki* cross-coupling reaction are crucial for the outcome of the reaction. Cross-coupling reactions of phenylboronic acid and its derivatives with 9,10-dibromoanthracene (**4**) have hitherto only been carried out with Na_2CO_3 as base and $[Pd(PPh_3)_4]$ as the catalyst in either toluene or a mixture of toluene and *THF* with good yields of 80 to 95% [8]. However, using this classical catalyst in *THF* and Na_2CO_3 as base for the coupling of **3** and **4** resulted in difficult removal of by-products such as phosphines and other decomposition products of the catalyst leading to lower yields of approx. 50%. To avoid this cumbersome purification step, the recently described, highly active catalyst bis(dicyclohexylamine)palladium acetate (*DAPCy*) was applied in ethanol with KOH as base [10]. This catalyst indeed proved to be a promising alternative producing higher yields of 79% of 9,10-bis(4-benzyloxyphenyl)anthracene (**5**) combined with a facilitated work up.

To obtain the desired product **6** cleavage of the benzyloxy group was attempted with several methods reported in literature such as the reduction with

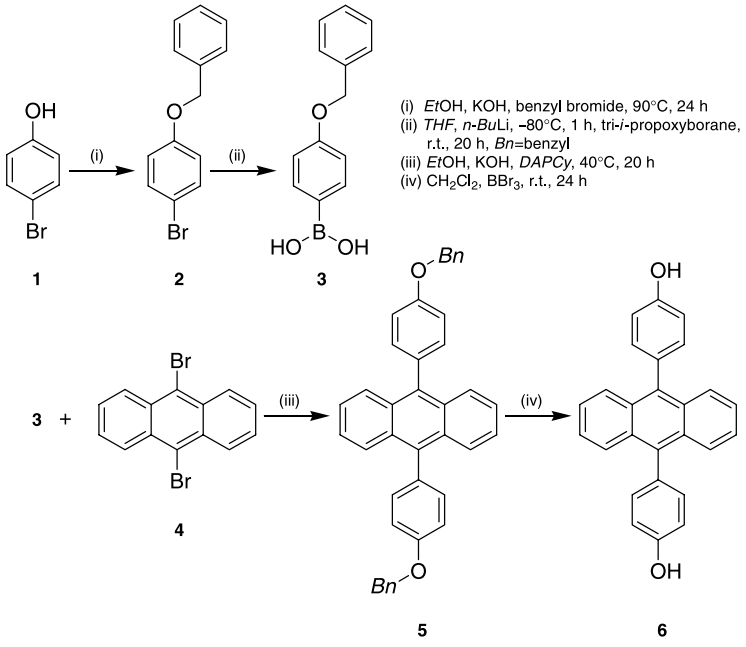

Scheme 1

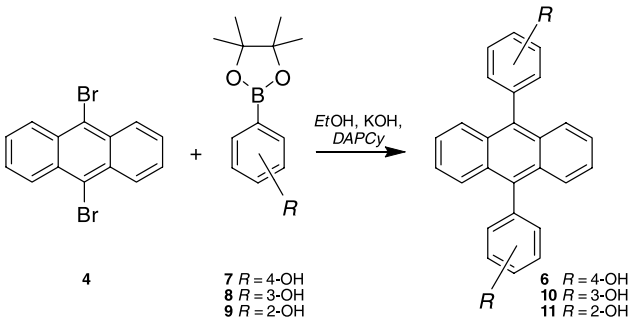

Scheme 2

1,4-cyclohexadien and Pd/C (10%) [11], with H_2 and Pd/C (10%) [8d], with elemental sodium in butanol [12], the dealkylation with BBr_3 in CH_2Cl_2 [8d, 11], and with KI in $BF_3 \cdot Et_2O$ [13]. Among these cleavage procedures, only the reaction with BBr_3 in CH_2Cl_2 gave a satisfying conversion yielding 47% of **6**.

Although the synthesis procedure described above was successful, the approach of *Chung et al.* [**8a**] making use of a methoxy protecting group and our approach utilizing the benzyloxy group for OH-protection suffer from the drawback of difficulties in removing the corresponding protecting group. Therefore, a synthesis route avoiding this yield-limiting step is desirable. As depicted in Scheme 2, our further attempts to prepare the 9,10-bis(hydroxyphenyl)anthracenes in a one-pot synthesis were based on the commercially available but much more expensive hydroxyphenyl pinacolboronates **7**–**9**. Indeed, we succeeded in the preparation of 9,10-bis(3-hydroxyphenyl)anthracene (**10**) in excellent yields of 95% using the *DAPCy* catalyst in *Et*OH and KOH, even though the corresponding *ortho*- and *para*-substituted derivatives **6** and **11** could not be obtained by this approach. It is worth noting that modifications of the synthesis procedure such as the use of the catalyst $[Pd(PPh_3)_4]$ instead of *DAPCy* or utilization of different solvents and solvent mixtures (toluene, *THF*, or ethanol/*THF*) did not improve the outcome of the reaction. However, the *meta*-derivative **10** was not only synthesized in high yields, but it was also easily purified by mere washing of the product with CH_2Cl_2 and acetone.

For a possible explanation of this somewhat unexpected behavior of the three different hydroxyphenyl pinacolboronates **7**–**9**, stereochemical effects of electron rich and electron deficient substituents on boronic acids have to be considered. However, reports on this very specific topic are scarce and so far most systematic studies focused on the influence of substituents on the aryl bromide component used in the *Suzuki* cross-coupling reaction [14]. A to some extent comparable study has been reported by *Prieto et al.* who coupled stereochemically different phenylboronic acids and phenylboronates bearing various substituents to indol derivatives [15]. Although they established some trends related to the nature of the substituent, their work compared only *ortho*- and *para*-substituted phenylboronic acids and does, therefore, not allow the establishment of a correlation to the effect observed here. From these publications it can be concluded that the yield of the cross-coupling reaction rises if the boronic acid bears substituents that push electrons to the aryl moiety. Thus, the nucleophilic character is increased making it a better reactant for the transmetalation step in the *Suzuki* reaction. Although steric effects on the differences in the reactivity of **7**–**9** must not be neglected, a strong influence of the electron donating character and the position of the hydroxy group can be anticipated. It has to be kept in mind that the reaction is performed under alkaline conditions using KOH as base. Consequently, the proton of the phenolic OH-function is withdrawn by this strong base, resulting in an anionic species as reactive agent. As proposed in Scheme 3 for the mesomeric forms of the boronates **7**–**9**, this anionic species is capable of delocalizing its negative charge over the whole aromatic ring, rendering the *ortho*- and *para*-position even more

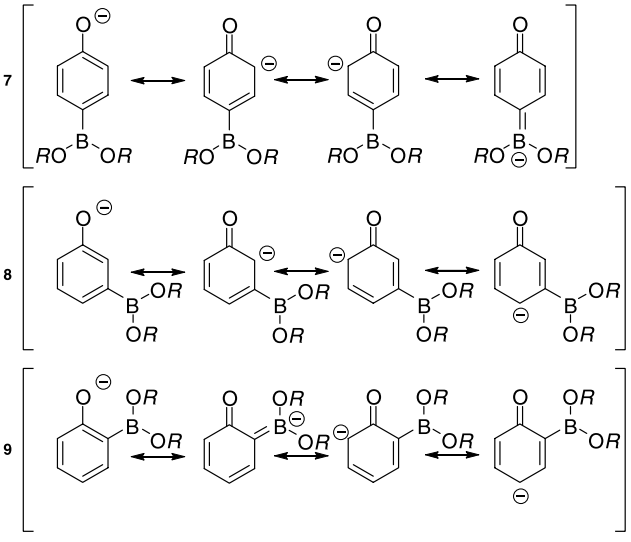

Scheme 3

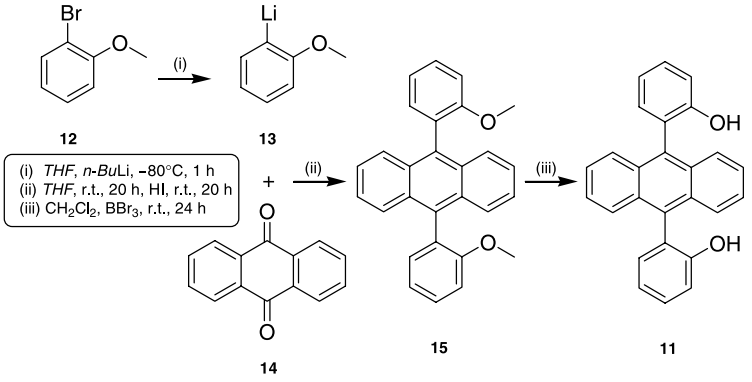

Scheme 4

nucleophilic [16]. However, the negative charge can also be withdrawn by the boron atom, thus giving rise to a less nucleophilic species, which also explains the significant number of undefined products observed during the *Suzuki* cross-coupling reaction of **4** with **7** and **9**. This proposed explanation is consistent with the high reactivity of **8** as it can be expected from the electron donating mesomeric effect of the phenolate group in the *meta*-position.

Since our attempts to obtain **11** directly from the boronate **9** failed, another pathway for its preparation had to be established. In order to give a general overview of possibilities to synthesize different 9,10-bis(hydroxyphenyl)anthracene derivatives, the aptness of a synthetic protocol coupling lithiumaryles to anthraquinone is herein described as shown in Scheme 4 [17]. Due to the strong alkaline media used for this reaction, the OH group was protected by the comparatively small methoxy group to avoid any possible sterical hindrance. Starting from 2-bromoanisol, the lithiated species was reacted with anthraquinone (**14**) to obtain **15** after work up with HI. Cleaving of the protecting group was again accomplished by BBr_3 in CH_2Cl_2 [8d, 11] giving **11** in pure form in a yield of 28%. Although a similar reaction was published by *Kwon et al.* giving considerable better yields [17], this procedure gave in our hands a number of unwanted by-products, which were hard to separate from **15**. Subsequent cleavage of the protecting group of crudely purified **15** turned out to facilitate the purification of the unprotected compound **11** due to its low solubility in apolar solvents.

To determine the photo physical properties of the compounds under investigation, UV-Vis absorption and photoluminescence (PL) measurements were performed in diluted solutions of methanol at room temperature under ambient conditions. Because it was assumed that deprotonation of the hydroxy group leads to significant changes in the electronic states of the molecules, *pH*-dependent absorption and emission spectra of the protonated and deprotonated species were investigated in neutral and alkaline environments (*cf.* Fig. 1 and Table 1). From literature it is known that anthracene displays a structured absorption spectrum that is mirrored by the structure of the fluorescence spectrum [18]. Further it has been reported that phenyl substituents on the position 9 and 10 of the anthracene core do not change the absorp-

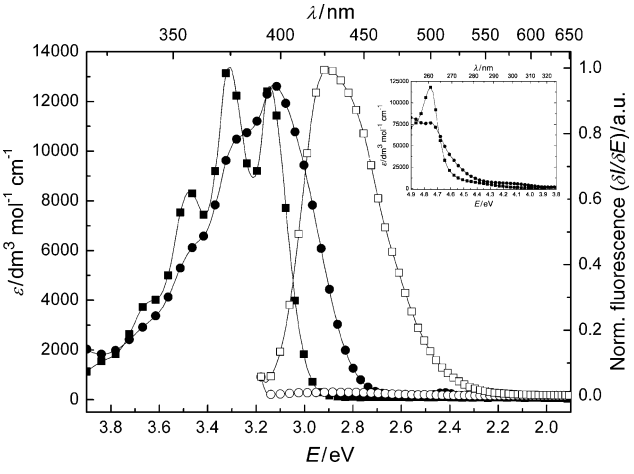

Fig. 1. Absorption and emission spectra of **6** in the protonated and deprotonated form recorded in *Me*OH. ■ Absorption of the protonated species, ● absorption upon addition of NaOH, □ emission of the protonated species ($\lambda_{exc} = 375$ nm) and ○ emission upon addition of NaOH. The inset shows the absorption spectra in the high energy region. Deprotonation was achieved by addition of 0.1 cm^3 NaOH solution (0.03 g in 1.5 cm^3 *Me*OH) to the diluted sample solutions. Further addition of base did not change the corresponding absorption and emission spectra

Table 1. Absorption (λ_{abs}) and emission wavelengths (λ_{em}) in solution of the protonated and deprotonated species recorded in methanol. The molecular coefficients of extinction for all compounds are in the same order of magnitude as shown for **6** in Fig. 1

Compound	Protonated		Deprotonated	
	λ_{abs}/nm	λ_{em}/nm	λ_{abs}/nm	λ_{em}/nm
Anthracene[a]	297, 309, 323 339, 356, 376	357, 397 420, 446	–	–
6	340, 357, 375, 395	423	360, 379, 397	~488
10	337, 355, 373, 393	421	341, 357, 375, 395	–[b]
11	339, 355, 373, 394	421	341, 357, 376, 396	–[b]

[a] Data taken from Ref. [18]; [b] **10** and **11** are not luminescent in their deprotonated forms

Table 2. INDO/SCI calculated transition energies (E), absorption maxima ($\lambda_{abs,calc}$), and oscillator strengths (OS) for the most relevant excited states in compounds **6**, **10**, and **11** in their ground-state equilibrium conformations

$-R^1/-R^2$	Compound	E/eV	$\lambda_{abs,calc}$/nm	OS	Dominant CI contribution
−OH/−OH	**6**	3.38	367	0.47	H → L
		4.80	258	1.25	H-3 → L, H → L + 1
		4.84	256	0.91	H → L + 3
	10	3.38	366	0.07	H → L + 1
		3.40	364	0.44	H → L
		4.82	257	1.99	H-3 → L
	11	3.40	365	0.06	H → L + 1
		3.44	360	0.39	H → L
		4.84	256	2.23	H-3 → L
$-O^-/-OH$	**6**	2.14	579	0.48	H → L
		3.40	365	0.15	H → L + 2, H-1 → L
		3.96	313	0.27	H → L + 5
		4.87	255	1.79	H-4 → L
	10	2.29	541	0.01	H → L
		3.22	386	0.41	H-1 → L
		4.77	260	1.29	H-4 → L
	11	2.30	540	0.14	H → L
		3.37	368	0.29	H-1 → L
		4.80	258	0.81	H-4 → L
		4.89	254	1.01	H-4 → L
$-O^-/-O^-$	**6**	2.46	503	0.48	H → L
		3.09	402	0.14	H → L + 1
		3.61	343	0.08	H-2 → L
		4.10	303	0.72	H → L + 3
		4.85	256	1.52	H-6 → L
	10	2.97	418	0.06	H → L
		3.28	378	0.41	H-2 → L
		3.85	322	0.22	H → L + 3
		4.74	261	0.49	H-4 → L
		4.84	256	0.47	several
		4.88	254	1.48	H-7 → L
	11	2.79	445	0.23	H → L
		3.28	378	0.12	H → L + 1
		3.44	361	0.19	H-2 → L
		3.74	331	0.27	H-1 → L + 4, H → L + 3
		4.46	278	0.42	H-1 → L + 5, H → L + 6
		4.84	256	0.27	H-2 → L + 3

tion and emission characteristics significantly, though the absorption and emission bands are broadened [8]. Additionally, aromatic compounds bearing hydroxy groups generally tend to shift their maxima to longer wavelengths combined with a loss of structural features of the corresponding spectra [8] and a *Stoke*'s shift dependent on the solvent polarity [19]. Comparing the absorption spectra of **6**, **10**, and **11** (*cf.* Table 1), only a slight broadening of the parental 9,10-diphenylanthracene structure [8] in the spectra of **10** and **11** is obtained upon deprotonation, whereas the three absorption peaks of **6** are noticeably broadened as shown in Fig. 1. Hence, the effect of deprotonation seems to be most striking when the hydroxy function is located *para* to the anthracene core. For the fluorescence spectra of **6**, **10**, and **11** a dramatic decrease of fluorescence intensity under alkaline conditions is observed for all compounds rendering the deprotonated species almost non fluorescent (*cf.* Fig. 1). Although upon deprotonation a red-shifted, very weak and broad emission maximum of **6** and **11** can be noticed, **10** does not show any luminescence under these experimental conditions. It is worth noting that a similar red-shifted emission band as the one obtained, *e.g.*, for **6** has been observed by *Chung et al.* for 9,10-bis(4-hydroxyphenyl)anthracene-ester derivatives [8a]. Photoluminescence quantum yields for all studied compounds were found to be around 80% for the fully protonated forms (experimental error ±7%) [18], while upon deprotonation quantum yields smaller than 1% were determined.

For a better understanding and explanation of the photo physical properties of the bis(hydroxyphenyl)anthracences, semi-empirical quantum mechanical calculations were performed (*cf.* Experimental) for the protonated as well as deprotonated species of **6**, **10**, and **11**. The transition energies, associated wavelengths, and oscillator strengths are summarized in Table 2 for compounds **6**, **10**, and **11** in their ground state equilibrium geometries for various degrees of deprotonation. As the present calculations only consider vertical transitions, the calculated transition energies correspond to the maximum of an envelope to the experimentally observed vibronic progressions.

The data for the fully protonated systems are consistent with the experimental observations. In particular, the energy of the first absorption maximum is largely unaffected by the position of the –OH sub-

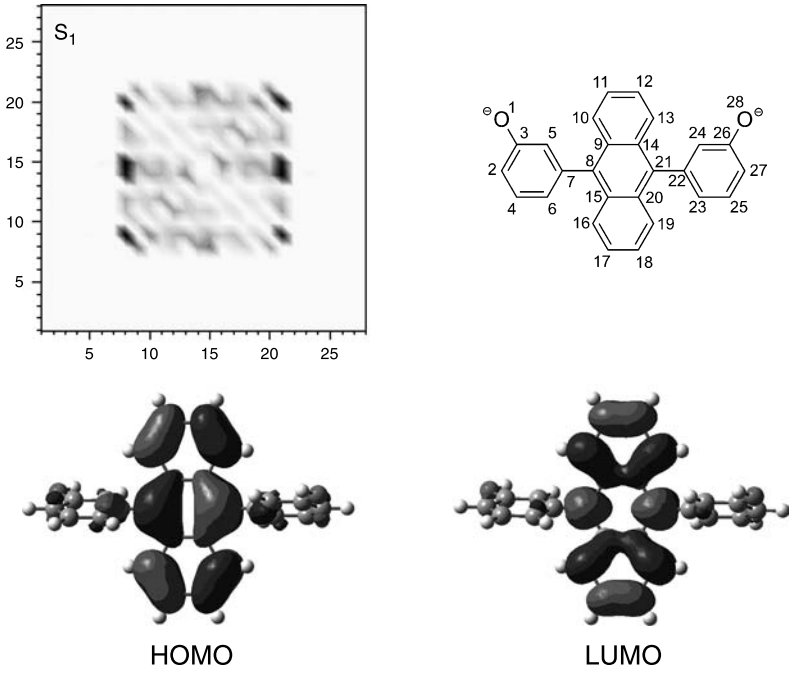

Fig. 2. Top left: INDO-SCI calculated electron-hole two-particle wavefunction for the lowest excited state in the fully protonated species of **10**. The shading gives the probability for finding the hole at the site denoted by x, while the electron is at the site denoted by y; top right: numbering of axes of the electron-hole two-particle wavefunction; bottom: illustrations of the HOMO and LUMO orbitals

stituent. This can be explained by the nature of the lowest optically allowed state of the fully protonated molecules. Its configuration interaction (CI) description is largely dominated by a HOMO → LUMO excitation with both orbitals localized strongly on the anthracene unit (*cf.* Fig. 2 for **10** as a typical example). Also the associated electron-hole two-particle wavefunction [20] shown in Fig. 2 confirms the localization of the exciton. There, the shading is proportional to the correlated probability for finding the hole at site x while the electron is at site y including the full CI description of the excited state. At higher energies, the calculations also well reproduce the strong peak(s) around 4.8 eV and the shoulder between 4.0 and 4.3 eV (the latter is related to two states not included in Table 2; they are described by excitations from the HOMO to higher-lying unoccupied orbitals).

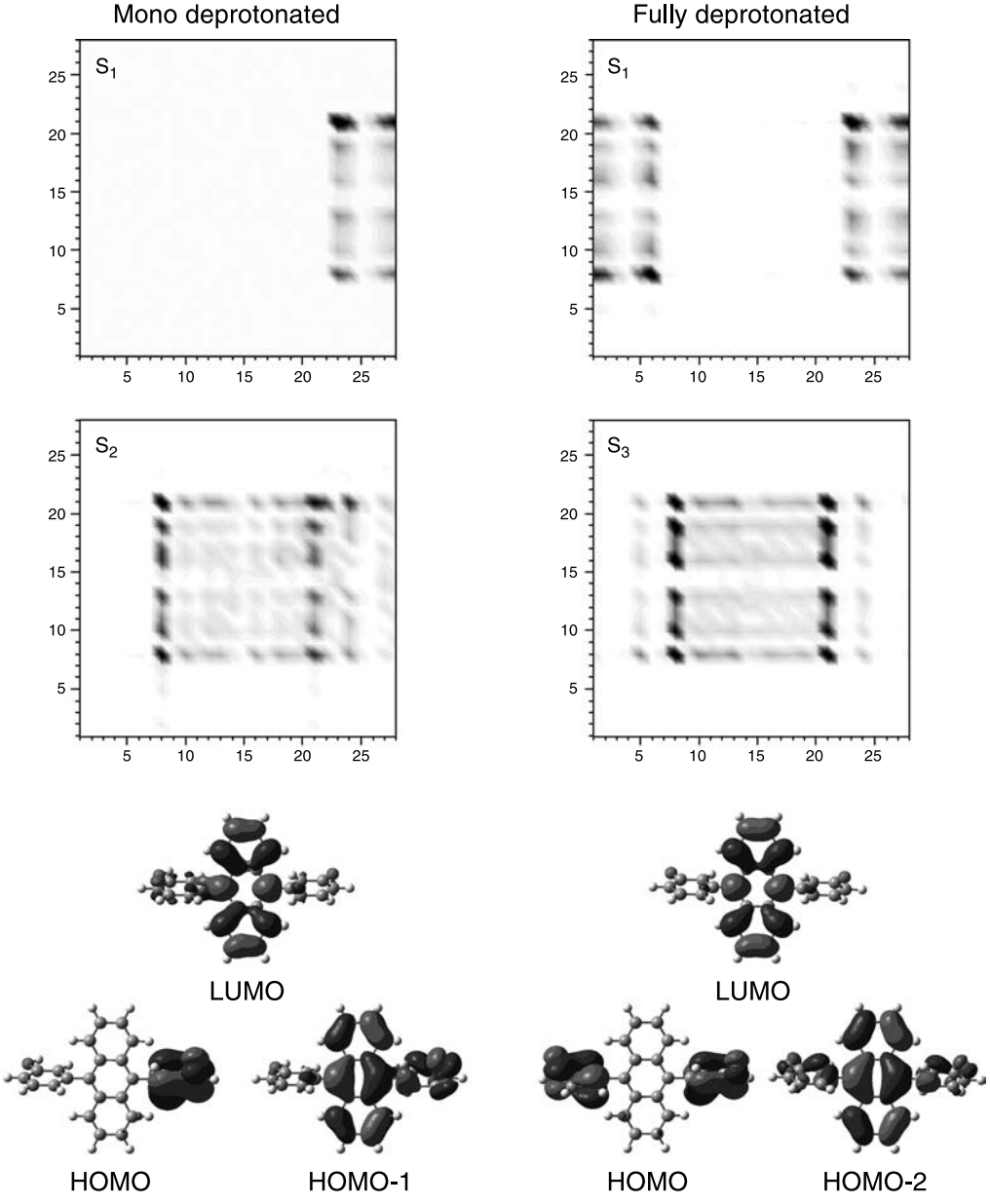

Fig. 3. Top: INDO-SCI calculated electron-hole two-particle wavefunction for the lowest excited state in the singly (left) and doubly (right) deprotonated species of **10**. The shading gives the probability for finding the hole at the site denoted by x, while the electron is at the site denoted by y (the numbering of the axes is the same as depicted in Fig. 2); center: electron-hole two particle wavefunction for first significantly allowed excited state; bottom: illustrations of the HOMO and LUMO orbitals

For the mono and fully deprotonated molecules, a strong red-shift of the lowest excited state is observed. With the exception of **10**, a significant oscillator strength is associated with the strongly red-shifted state(s), which is not consistent with the experimental observations. This cannot be directly related to the applied semi-empirical methodology, as when instead using density functional based methods for geometry optimization and excitation energy calculation the deviations are even larger. Thus, in the following, we will adopt a dual strategy: first, the results for **10**, with the –OH groups in *meta* position will be discussed and, subsequently, based on these results, the presumable origin of the deviations for **6** and **11** will be elucidated.

In the mono (fully) deprotonated form of **10**, the lowest-lying excited state at 2.29 (2.97) eV is characterized by a vanishing oscillator strength and the first allowed state at 3.22 (3.28) eV is only slightly red-shifted compared to the fully protonated molecule. This small shift of the absorption maximum is in excellent agreement with the experimental observation. The low-lying optically forbidden state, on the other hand, is responsible for the molecules becoming non-emissive in the deprotonated form. To more accurately describe the emission process, we have also calculated the equilibrium geometries of the excited molecules. For the fully protonated form of **10**, we find the lowest excited state shifted to 2.99 eV (414 nm; $OS = 0.56$), while for the mono and fully deprotonated molecules optically forbidden states at 1.99 eV (622 nm; $OS = 0.00$) and 2.68 eV (462 nm; $OS = 0.03$) are lowest in energy. Based on this good correlation between experimental and theoretical results for **10**, a more in depth analysis of the nature of the various states in the deprotonated molecule was performed. As shown in Fig. 3, the LUMO in the deprotonated molecule is strongly reminiscent of that of the protonated one. The HOMO, however is localized on the ring(s) bearing the $-O^-$ group(s). As a consequence, the lowest excited state, which is dominantly described by a HOMO to LUMO excitation (*cf.* Table 2) possesses a pronounced charge transfer character. This is also confirmed by the electron-hole two-particle wavefunctions (which contain the full CI-based information of the excited state going beyond the simple orbital picture) in the top part of Fig. 3. They clearly show that the hole is confined to the deprotonated ring(s), while the electron is localized on the anthracene backbone. The vanishing overlap between electron and hole is also responsible for the vanishing oscillator strength and resulting strongly increased radiative lifetime associated with the lowest excited state. The first optically allowed state, S_2 for the mono (S_3 for the fully) deprotonated molecule, is described by an excitation from the HOMO-1 (HOMO-2) to the LUMO. The respective orbitals are similar to the HOMO of the fully protonated system, the main difference being that they somewhat extend onto the deprotonated ring(s). The conclusions drawn from the orbital pictures are again confirmed by the electron-hole wavefunctions. Consequently, this state is closely related to the first optically allowed state in the fully protonated molecule. The overall picture developed above, provides a consistent explanation for the experimental observation that the emission from **10** is fully quenched upon deprotonation, while the optical absorption spectra are only slightly modified.

Considering the experimental data, a similar behavior as for **10** should also be expected for **6** and **11**. Indeed, also there the lowest excited state possesses a significant charge transfer character. The main difference compared to the above described situation is the relatively high oscillator strength of that state, which should render the deprotonated forms of **6** and **11** emissive. The reason is that in **6** and **11** the degree of localization of the HOMO on the deprotonated ring(s) is less pronounced than for **10**, which is presumably related to the $-O^-$ groups in the *ortho*- and *para*-positions. This results in a stronger overlap between the electron and hole (in the simple orbital picture between LUMO and HOMO) and consequently a larger transition dipole. To understand the origin of this behavior, we have calculated the electronic structure for the ground and excited states in the fully deprotonated form of **6** as a function of the twist angle between the anthracene and the two phenyl rings. The corresponding transition energies, oscillator strengths, and orbitals are shown in Fig. 4. From these plots it becomes obvious that a decreased coupling between the anthracene core and the phenyl rings (achieved here by increasing the twist) would yield the desired results by localizing the orbitals more strongly, significantly decreasing the oscillator strength of the lowest excited state (rendering the material essentially non-emissive) and recovering the oscillator strength of the state in the region of the first absorption peak of the fully protonated molecule. The overestimation of the coupling in our calcula-

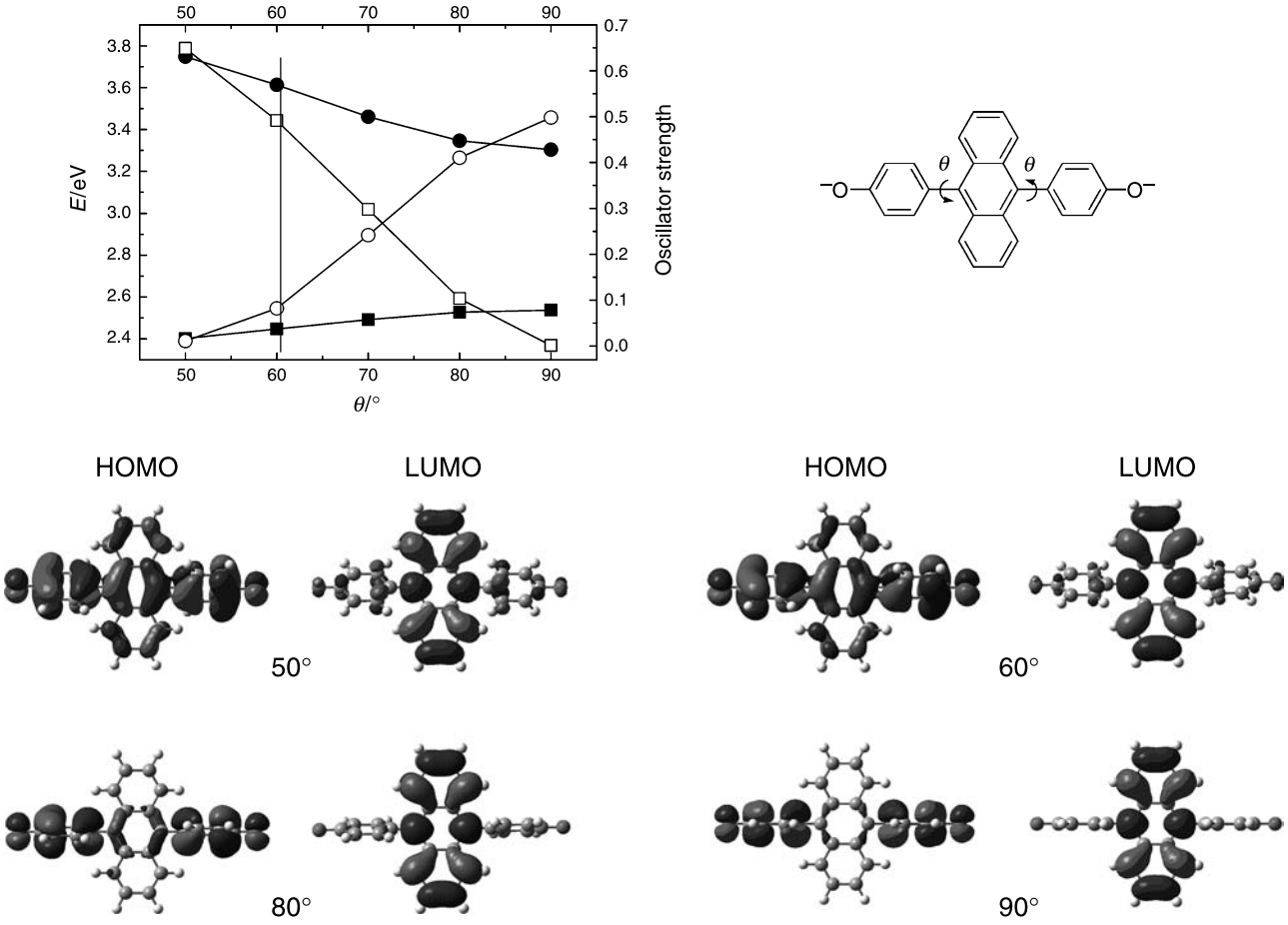

Fig. 4. Fully deprotonated molecule **6**. Top left: INDO/SCI calculated change of excited state energies (filled symbols) and oscillator strengths (open symbols) as a function of the twist angle θ for the lowest excited state (squares) and the state corresponding to the main peak in the fully protonated species (circles, details see text). The vertical line at 60.4° corresponds to the twist in the fully relaxed molecule. The HOMOs and LUMOs for selected twist angles are also shown. Note that the twists are applied synchronously

tions on the fully geometry optimized molecules of **6** and **11** is tentatively attributed to a combination of factors including solvent effects and the interaction with counter ions in solution.

Conclusion

In this contribution three different synthesis routes for the preparation of 9,10-bis(4-hydroxyphenyl)anthracene (**6**), 9,10-bis(3-hydroxyphenyl)anthracene (**10**), and 9,10-bis(2-hydroxyphenyl)anthracene (**11**) were presented giving these materials in good to acceptable yields of 47, 95, and 28%. Further, the photo physical properties in solution and the effects of deprotonation on absorption and emission spectra were discussed and explained *via* quantum mechanical calculations.

Experimental

Unless otherwise noted, materials were obtained from commercial sources (Aldrich, Fluka or Lancaster) and were used without further purification. Solvents for reactions were freshly distilled over appropriate drying agents prior to use. Reactions were carried out under inert atmosphere of Ar using standard *Schlenk* techniques. ^{1}H NMR spectra were recorded on a Varian INOVA 500 MHz Spectrometer at 500 MHz, ^{13}C{^{1}H} NMR spectra were recorded at 125 MHz. Assignment of the peaks was done by DEPT and COSY NMR spectroscopy. Solvent residual peaks were used for referencing the NMR spectra to the corresponding values given in literature [21]. Elemental analyses (C and H) were conducted for the novel compounds **5** and **10** with results that were found to be in good agreement ($\pm$0.2%) with the calculated values. UV-Visible absorption spectra were recorded on a Cary 50 Bio UV-Visible Spectrophotometer, fluorescence spectra on a Perkin Elmer Luminescence Spectrometer LS50B. PL quantum yields were measured using a Shimadzu RF-5301PC

Spectrofluorimeter (detector corrected) and Perkin Elmer Lambda 9 UV/VIS/NIR Spectrophotometer using quinine sulphate dihydrate in 0.1 *N* H_2SO_4 as standard.

Quantum mechanical calculations consisted of the optimization of molecule geometries in their ground state using the semi-empirical *Hartree-Fock* Austin Model 1 (AM1) method [22] as implemented in Ampac6.55. For optimizing the geometries of the lowest excited states, the AM1 Hamiltonian was coupled to a single configuration interaction (SCI) scheme [23] including 7 occupied and 7 unoccupied orbitals in the CI active space (necessary for avoiding an artificial symmetry breaking at all levels of deprotonation). Transition energies and oscillator strengths were calculated on the basis of the semi-empirical *Hartree-Fock* intermediate neglect of differential overlap method. Electron correlation effects were also here included *via* SCI (26 × 26 active orbitals) [24]. These calculations were performed on the one hand using a slightly modified version of the original ZINDO code by *Zerner* and coworkers as well as using Gaussian 98 (Revision A.9) [25]. Consistent results were obtained with both codes. Electron-hole two-particle wavefunctions were calculated using Zoa 2.5. [26]. Gaussian 98 (Revision A.11) was used for the comparative density-functional theory based calculations.

4-Benzyloxybromobenzene (**2**)
As an alternative to the procedure of *Kim et al.* [9c], 10.4 g **1** (60.2 mmol) were dissolved in a mixture of 70 cm^3 aqueous KOH solution (2 *M*) and 140 cm^3 ethanol. After heating to 90°C, 16 cm^3 benzyl bromide (134.5 mmol) were added followed by refluxing the reaction mixture for 24 h at that temperature. Cooling to room temperature and stripping of the aqueous phase yielded a white solid which was dried and further purified by column chromatography on silica (*cy*:*ee* = 5:1). Sampling the band at $R_f = 0.67$ (*cy*:*ee* = 4:1) gave 14.0 g (88%) **2**. ^{1}H and ^{13}C NMR spectra were found to be identical with the ones described in Ref. [9c].

4-Benzyloxyphenylboronic acid (**3**)
Compound **3** was prepared according to *Gimeno et al.* with ^{1}H NMR spectra as reported in Ref. [9d].

9,10-Bis(4-benzyloxyphenyl)anthracene (**5**, $C_{40}H_{30}O_2$)
Compound **4** (0.98 g, 2.9 mmol), 1.64 g **3** (7.2 mmol), and 0.50 g KOH (8.9 mmol) were dissolved in 55 cm^3 ethanol under Ar. For acceleration of the dissolving process, the mixture was treated with ultrasound for 1 min. After addition of 0.01 g of the catalyst *DAPCy* (0.02 mmol), the reaction mixture was stirred at 40°C for 20 h during which precipitation of the product occurred. The precipitate was isolated by filtration, washed with 5 cm^3 methanol, and recrystallized from CH_2Cl_2 several times yielding 1.25 g (79%). $R_f = 0.66$ (*cy*:*ee* = 4:1). ^{1}H NMR (500 MHz, $CDCl_3$): $\delta = 7.75$ (dd, $J = 6.8$, 3.4 Hz, 4H, $Ant^{1,4,5,8}$), 7.56 (d, $J = 7.3$ Hz, 4H, $Bn^{2,6}$), 7.46 (t, $J = 7.3$ Hz, 4H, $Bn^{3,5}$), 7.44–7.32 (m, 2H, Bn^4), 7.40 (d, $J = 8.8$ Hz, 4H, $Ph^{3,5}$), 7.33 (dd, $J = 6.8$, 3.4 Hz, 4H, $Ant^{2,3,6,7}$), 7.22 (d, $J = 8.8$ Hz, 4H, $Ph^{2,6}$), 5.22 (s, 4H, OCH_2) ppm; ^{13}C NMR (125 MHz, $CDCl_3$): $\delta = 158.3$ (2C, Ph^4), 137.0, 136.7 (4C, $Ant^{9,10}$, Bn^1), 132.4 (4C, $Ph^{2,6}$), 131.4 (2C, Ph^1), 130.2 (4C, $Ant^{4a,8a,9a,10a}$), 128.7 (4C, $Bn^{3,5}$), 128.1 (2C, Bn^4), 127.6 (4C, $Bn^{2,6}$), 127.0 (4C, $Ant^{1,4,5,8}$), 124.9 (4C, $Ant^{2,3,6,7}$), 114.7 (4C, $Ph^{3,5}$), 70.2 (2C, OCH_2) ppm.

9,10-Bis(4-hydroxyphenyl)anthracene (**6**)
Compound **5** (0.40 g, 0.7 mmol) was suspended in 10 cm^3 dry CH_2Cl_2 under Ar and treated with ultrasound for 1 min. To the dirty-white suspension, 0.7 cm^3 BBr_3 (1 *M*, 0.7 mmol) were added drop wise followed by stirring at room temperature for 24 h. After addition of 30 cm^3 H_2O, the reaction mixture was acidified with 2 cm^3 aqueous HCl solution (10%) and stirred for further 24 h. The product was extracted four times with 70 cm^3 CH_2Cl_2 from H_2O, dried (Na_2SO_4), and purified by recrystallization from little CH_2Cl_2 several times yielding 0.13 g (47%) of a weakly brown colored powder. $R_f = 0.14$ (*cy*:*ee* = 4:1). ^{1}H NMR (500 MHz, $CDCl_3$): $\delta = 8.66$ (s, 2H, *OH*), 7.74 (dd, $J = 6.8$, 3.0 Hz, 4H, $Ant^{1,4,5,8}$), 7.38 (dd, $J = 6.8$, 3.0 Hz, 4H, $Ant^{2,3,6,7}$), 7.29 (d, $J = 8.3$ Hz, 4H, $Ph^{2,6}$), 7.13 (d, $J = 8.3$ Hz, 4H, $Ph^{3,5}$) ppm; ^{13}C NMR (125 MHz, $CDCl_3$): $\delta = 158.6$ (2C, Ph^4), 138.5 (2C, $Ant^{9,10}$), 133.8 (4C, $Ph^{2,6}$), 131.9 (4C, $Ant^{4a,8a,9a,10a}$), 131.2 (2C, Ph^1), 128.5 (4C, $Ant^{1,4,5,8}$), 126.5 (4C, $Ant^{2,3,6,7}$), 117.0 (4C, $Ph^{3,5}$) ppm; UV-Vis (methanol): $\lambda_{abs,protonated} = 340$, 357, 375, 395 nm, $\lambda_{abs,deprotonated} = 360$, 379, 397 nm; fluorescence (methanol): $\lambda_{em,protonated} = 423$ nm, $\lambda_{em,deprotonated} =$ around 488 nm (broad and weak). Spectra were found to be in accordance with Ref. [8].

9,10-Bis(3-hydroxyphenyl)anthracene (**10**, $C_{26}H_{18}O_2$)
Compound **4** (0.30 g, 0.9 mmol), 0.47 g **8** (2.1 mmol), and 0.18 g KOH (3.2 mmol) were dissolved in 20 cm^3 ethanol under Ar. For acceleration of the dissolving process, the mixture was treated with ultrasound for 1 min. After the addition of 0.005 g of the catalyst *DAPCy* (0.01 mmol), the reaction was stirred at 40°C for 24 h. The reaction mixture was filtered over Celite® followed by elution of the product with methanol. Evaporation of the solvent and treatment with CH_2Cl_2 and methanol gave a suspension which was filtrated. The residue was washed with acetone several times yielding 0.31 g (95%) **10** as white powder. $R_f = 0.20$ (*cy*:*ee* = 4:1). ^{1}H NMR (500 MHz, CD_3OD): $\delta = 7.71$ (dd, $J = 6.8$, 3.4 Hz, 4H, $Ant^{1,4,5,8}$), 7.38 (t, $J = 7.8$ Hz, 2H, Ph^5), 7.29 (dd, $J = 6.8$, 3.4 Hz, 4H, $Ant^{2,3,6,7}$), 6.96 (dd, $J = 8.3$, 2.4 Hz, 2H, Ph^6), 6.84 (dd, $J = 2.4$ Hz, 2H, Ph^2), 6.80 (d, $J = 7.3$ Hz, 2H, Ph^4), 4.85 (s, 2H, *OH*) ppm; ^{13}C NMR (125 MHz, CD_3OD): $\delta = 160.8$ (2C, Ph^3), 141.6 (2C, Ph^1), 138.5 (2C, $Ant^{9,10}$), 131.0 (4C, $Ant^{4a,8a,9a,10a}$), 130.4 (2C, Ph^5), 128.0 (4C, $Ant^{1,4,5,8}$), 125.8 (4C, $Ant^{2,3,6,7}$), 122.3 (2C, Ph^6), 120.1 (2C, Ph^4), 116.3 (2C, Ph^2) ppm; UV-Vis (methanol): $\lambda_{abs,protonated} = 337$, 355, 373, 393 nm, $\lambda_{abs,deprotonated} = 341$, 357, 375, 395 nm; fluorescence (methanol): $\lambda_{em,protonated} = 421$ nm.

9,10-Bis(2-methoxyphenyl)anthracene (**15**)
Compound **12** (0.56 g, 3.0 mmol) was dissolved in 20 cm^3 anhydrous *THF* under Ar and cooled to −80°C. *n*-Butyl lithium (2 cm^3, 2.5 *M* in hexane, 5.0 mmol) were added drop wise followed by stirring the reaction mixture at −80°C for 1 h. After addition of 0.26 g **14** (1.2 mmol), the reaction was allowed to attain room temperature and stirred for further 20 h.

HI (1.8 cm^3, ~55%, 13.0 mmol) was added followed by stirring for another 20 h. Work up consisted of adding 70 cm^3 H_2O, 3 cm^3 $Na_2S_2O_3$ (2%), 1 cm^3 aqueous HCl solution (10%), and the subsequent extraction with CH_2Cl_2. The solvent was evaporated and the residue purified by column chromatography on silica (*cy*:*ee* = 30:1). Sampling the band at $R_f = 0.75$ (*cy*:*ee* = 4:1) gave 0.03 g (3%) **15** as a slightly yellow powder. ^{1}H NMR (500 MHz, $CDCl_3$): $\delta = 7.63$ (dd, $J = 6.8$, 3.4 Hz, 4H, *Ant*^{1,4,6,8}), 7.58–7.51 (m, 2H, *Ph*^{6}), 7.36 (dd, $J = 7.3$, 1.9 Hz, 2H, *Ph*^{4}), 7.30 (dd, $J = 6.8$, 3.4 Hz, 4H, *Ant*^{2,3,6,7}), 7.22–7.14 (m, 4H, *Ph*^{3,5}), 3.66 (s, 6H, *OCH*$_3$) ppm; ^{13}C NMR (125 MHz, $CDCl_3$): $\delta = 158.1$ (2C, *Ph*^{2}), 133.6 (2C, *Ant*^{9,10}), 130.1 (4C, *Ant*^{4a,8a,9a,10a}), 129.2 (2C, *Ph*^{6}), 128.8 (2C, *Ph*^{4}), 127.7 (2C, *Ph*^{1}), 126.9 (4C, *Ant*^{1,4,5,8}), 124.7 (4C, *Ant*^{2,3,6,7}), 120.7 (2C, *Ph*^{5}), 111.2 (2C, *Ph*^{3}), 55.7 (2C, O*CH*$_3$) ppm. Spectra were found to be in accordance with Ref. [17].

9,10-Bis(2-hydroxyphenyl)anthracene (**11**)
Compound **15** (0.015 g, 0.04 mmol) was dissolved in 4 cm^3 dry CH_2Cl_2 under Ar. BBr_3 (0.5 cm^3, 1 *M*, 0.5 mmol) was added followed by stirring the reaction mixture at room temperature for 24 h. After addition of 60 cm^3 H_2O, the reaction mixture was acidified with 2 cm^3 aqueous HCl solution (10%) and stirred for further 24 h. The product was extracted four times with 50 cm^3 CH_2Cl_2 from H_2O, dried (Na_2SO_4), and purified by column chromatography on silica (*cy*:*ee* = 10:1). Sampling the band at $R_f = 0.36$ (*cy*:*ee* = 4:1) gave 0.004 g (28%) **11**. ^{1}H NMR (500 MHz, $(CD_3)_2CO$): $\delta = 8.03$–8.00 (m, 2H, *OH*), 7.73–7.67 (m, 4H, *Ant*^{1,4,5,8}), 7.50–7.43 (m, 2H, *Ph*^{6}), 7.41–7.34 (m, 4H, *Ant*^{2,3,6,7}), 7.30–7.23 (m, 2H, *Ph*^{4}), 7.22–7.16 (m, 2H, *Ph*^{3}), 7.16–7.09 (m, 2H, *Ph*^{5}) ppm; UV-Vis (methanol): $\lambda_{abs,protonated} = 339$, 355, 373, 394 nm, $\lambda_{abs,deprotonated} = 341$, 357, 376, 396 nm; fluorescence (methanol): $\lambda_{em,protonated} = 421$ nm. Spectra were found to be in accordance with Ref. [17].

Acknowledgements

Financial support by the Austrian Science Fund in the framework of the Austrian Nano Initiative RPC ISOTEC – RP 0701 and 0702 is gratefully acknowledged.

References

[1] For examples see: a) de Silva AP, Gunaratne HQN, Gunnlaugsson T, Huxley AJM, McCoy CP, Rademacher JT, Rice TE (1997) Chem Rev **97**: 1515; b) Balzani V, Credi A, Raymo FM, Stoddart JF (2000) Angew Chem Int Ed **39**: 3348; c) Charier S, Ruel O, Baudin J-B, Alcor D, Allemand J-F, Meglio A, Jullien L, Valeur B (2006) Chem Eur J **12**: 1097
[2] a) Mancin F, Rampazzo E, Tecilla P, Tonellato U (2006) Chem Eur J **12**: 1844; b) Wang Z, Zheng G, Lu P (2005) Org Lett **7**: 3669
[3] Werts MHV, Gmouh S, Mongin O, Pons T, Blanchard-Desce M (2004) J Am Chem Soc **126**: 16294
[4] a) Yang WJ, Kim DY, Jeong M-Y, Kim HM, Lee YK, Fang X, Jeon S-J, Cho BR (2005) Chem Eur J **11**: 4191; b) Kim Y-H, Jeong H-C, Kim S-H, Yang K, Kwon S-K (2005) Adv Funct Mater **15**: 1799
[5] Desvergne J-P, Lahrahar N, Gotta M, Zimmermann Y, Bouas-Laurent H (2005) J Mater Chem **15**: 2873
[6] Basaric N, Wan P (2006) J Org Chem **71**: 2677
[7] Suzuki A (2005) Chem Commun 4759
[8] a) Chung S-J, Kim K-K, Jin J-I (1999) Polymer **40**: 1943; b) Kotha S, Ghosh AK, Deodhar KD (2004) Synthesis 549; c) Kotha S, Ghosh AK (2002) Synlett 451; d) Wagner G, Herrmann R, Scherer W (1996) J Organomet Chem **516**: 225; e) Hu D, Fuh RA, Li J, Corkan A, Lindsey JS (1998) Photochem Photobiol **68**: 141
[9] a) Sharma SK, Kanamathareddy S, Gutsche CD (1997) Synthesis **11**: 1268; b) Geng Y, Trajkovska A, Katsis D, Ou JJ, Culligan SW, Chen SH (2002) J Am Chem Soc **124**: 8337; c) Kim J, Kim YK, Park N, Hahn JH, Ahn KH (2005) J Org Chem **70**: 7087; d) Gimeno N, Ros MB, Serrano JL, de la Fuente MR (2004) Angew Chem Int Ed **43**: 5235
[10] a) Tao B, Boykin DW (2004) J Org Chem **69**: 4330; b) Kappaun S, Zelzer M, Bartl K, Saf R, Stelzer F, Slugovc C (2006) J Polym Sci Part A Polym Chem **44**: 2130; c) Kappaun S, Sovic T, Stelzer F, Pogantsch A, Zojer E, Slugovc C (2006) Org Biomol Chem **4**: 1503
[11] Kocienski PJ (1994) Protecting Groups, Georg Thieme Verlag, Stuttgart
[12] Loev B, Dawson CR (1956) J Am Chem Soc **78**: 6095
[13] Vankar YD, Rao CT (1985) J Chem Research (S): 232
[14] For examples see: a) Bandgar BP, Bettigeri SV, Phopase J (2004) Org Lett **6**: 2105; b) Edsall RJJ, Harris HA, Manas ES, Mewshaw RE (2003) Bioorg Med Chem **11**: 3457
[15] Prieto M, Zurita E, Rosa E, Munoz L, Lloyd-Williams P, Giralt E (2004) J Org Chem **69**: 6812
[16] Beyer H, Walter W (1998) Lehrbuch der Organischen Chemie, S. Hirzel Verlag, Stuttgart
[17] a) Kwon SK, Kim YH, Shin SC (2002) Bull Korean Chem Soc **23**: 17; b) Stoessel P, Breuning E, Vestweber H, Heil H (2006) PCT Int Appl, WO 2006048268 A1
[18] a) Valeur B (2001) Molecular Fluorescence – Principles and Applications, Wiley-VCH, Weinheim; b) Lakowicz JR (1999) Principles of Fluorescence Spectroscopy, Kluwer Academic/Plenum Publishers, New York; c) Morris JV, Mahaney MA, Huber JR (1976) J Phys Chem **80**: 969; d) Kim Y-H, Kwon S-K (2006) J Appl Polym Sci **100**: 2151
[19] Tautges A (2002) J Phys Chem Lab **4**: 8
[20] Here we follow the definition given in Romaner L, Heimel G, Wiesenhofer H, Scandiucci de Freitas P, Scherf U, Brédas JL, Zojer E, List EJW (2004) Chem Mater **16**: 4667 rather than applying the symmetrized version we used in previous works
[21] Gottlieb HE, Kotylar V, Nudelman A (1997) J Org Chem **62**: 7512
[22] Dewar MJS, Zoebisch EG, Healy EF, Stewart JJP (1985) J Am Chem Soc **107**: 3902
[23] Ampac 5.0 User's Manual (1994) Copyright Semichem, 7128 Summit, Shwanee, KS 66216

[24] a) Pople JA, Beveridge DL, Dobosh PA (1967) J Chem Phys **47**: 2026; b) Ridley J, Zerner M (1973) Theoret Chim Acta **32**: 111

[25] Gaussian 98, Revision A.9, Frisch MJ, Trucks GW, Schlegel HB, Scuseria GE, Robb MA, Cheeseman JR, Zakrzewski VG, Montgomery JA, Stratmann RE, Burant JC, Dapprich S, Millam JM, Daniels AD, Kudin KN, Strain MC, Farkas O, Tomasi J, Barone V, Cossi M, Cammi R, Mennucci B, Pomelli C, Adamo C, Clifford S, Ochterski J, Petersson GA, Ayala PY, Cui Q, Morokuma K, Malick DK, Rabuck AD, Raghavachari K, Foresman JB, Cioslowski J, Ortiz JV, Baboul AG, Stefanov BB, Liu G, Liashenko A, Piskorz P, Komaromi I, Gomperts R, Martin RL, Fox DJ, Keith T, Al-Laham MA, Peng CY, Nanayakkara A, Challacombe M, Gill PMW, Johnson B, Chen W, Wong MW, Andres JL, Gonzalez C, Head-Gordon M, Replogle ES, Pople JA (1998) Gaussian Inc., Pittsburgh PA

[26] Zoa v2.0, Calbert JP, Service de Chimie des Matériaux Nouveaux, Mons (Belgium), options 3D and not anti-symmetrized